Deformation and dissipated energies for high cycle fatigue of 2024-T3 aluminium alloy

S. Giancane, Andre Chrysochoos, V. Dattoma, Bertrand Wattrisse

Deformation and dissipated energies for high cycle fatigue of 2024-T3 aluminium alloy

S. Giancane [a,*], A. Chrysochoos [b], V. Dattoma [a], B. Wattrisse [b]

[a] Dipartmento di Ingegneria dell'Innovazione, Università del Salento, via per Arnesano, 73100 Lecce, Italy
[b] Laboratoire de Mechanique et Génie Civil, Université de Montpellier II (France) 860, route de St. Priest 34090 Montpellier, France

During the high cycle fatigue of aluminium alloys, an energy dissipation occurs. This dissipation is hard to be estimated because of the high diffusivity of such alloys and the importance of the thermoelasticity effects in comparison with others standard metallic materials (e.g., steels). Nevertheless the study of the energy balance gives valuable information about the nature of deformation mechanisms facilitating the construction of constitutive models associated with the microplasticity and damage of the aluminium alloy. In this work, the different energies involved in the energy balance were deduced from two complementary imaging techniques. The dissipation and thermoelastic sources were derived from an infrared thermography system, while the deformation energy was estimated from a digital image correlation system. Three tests with various loading blocks were carried out and a comparison between deformation and dissipation energies was systematically performed.

1. Introduction

The mechanical response of materials subjected to fatigue loading is a statistical phenomenon and depends on a series of different factors that makes it impossible to estimate the duration of a mechanical component without a negligible uncertainty. Moreover the localization of fatigue damage is a stochastic process if notches or some preferential crack path are not present. Indeed, only in the very first part of lifespan of the material the response can be considered as homogeneous, because damage gradually develops until a damaged zone preferentially grows, leading the component to cracking and rupture.

Fatigue phenomena are cumulative, irreversible mechanisms. They dissipate the deformation energy into the material leading to a self-heating of the specimen. The associated heat sources can then be estimated to track the potential zones where plasticity and damage preferentially develops [1–4].

In this work, digital image correlation (DIC) [5–8] and infrared thermography (IRT) [1–4,9,10] were used to study the fatigue behavior of an aluminium alloy 2024 T3. DIC allows the deformation energy over one cycle to be computed while the infrared data are used to estimate through the heat diffusion equation the thermoelastic and dissipation sources accompanying the fatigue loading. Both are non-destructive and non-intrusive imaging techniques which allow, under some conditions, the deformation and dissipation energies to be computed and compared at the same time on a same material zone. Indeed for fatigue test, the mechanical energy over a cycle involves the dissipation, the internal energy variation and the possible effects of the thermomechanical coupling. In the case of aluminium 2024 T3, the influence of thermoelastic coupling on the mechanical hysteresis loop size is negligible and the deformation energy is then only due to the dissipated energy and the internal energy variations.

The goal of this work is then the comparison of both energies using independent and complementary experimental approaches. The paper is composed as follows: the expression of the heat diffusion equation and the definition of the different heat sources are first briefly reviewed. The image processing method is then described. The methods developed to compute the deformation energy and the heat sources are shown. A comparison between deformation and dissipation energies is finally proposed for different series of loading blocks.

2. Theoretical framework

In order to interpret the experimental results it is necessary to define a theoretical framework. In this section, starting from the irreversible process thermomechanics of continuous media, the heat equation and the different heat sources accompanying the fatigue development are briefly reminded and some hypotheses and necessary approximations are proposed. Moreover an analysis for the energy balance associated with a load cycle is proposed.

* Corresponding author. Tel.: +39 (0)832 297786; fax: +39 (0)832 297768.
E-mail address: simone.giancane@unile.it (S. Giancane).

The reader interested in a detailed presentation of these thermomechanical aspects is invited to refer to [1–4,11,12].

2.1. Thermomechanical approach

Considering a homogeneous, isotropic material, the local heat equation can be written as

$$\rho C\dot{T} - \mathrm{div}(k\,\mathrm{grad}T) = \left(\sigma - \rho\frac{\partial\psi}{\partial\varepsilon}\right) : \dot{\varepsilon} - \rho\frac{\partial\psi}{\partial\alpha}\cdot\dot{\alpha} + \rho T\frac{\partial^2\psi}{\partial T\partial\varepsilon} : \dot{\varepsilon} + \rho T\frac{\partial^2\psi}{\partial T\partial\alpha}\cdot\dot{\alpha} + r_e \quad (1)$$

where the involved terms have the following physical significance:

- $\rho C\dot{T}$ represents the stored (or released) heat rate; in what follows, we will suppose that ρ and C are material constants.
- $-\mathrm{div}(k\mathrm{grad}T)$ is the heat rate losses by conduction; for homogeneous isotropic material, k is a constant and $-\mathrm{div}\,(k\,\mathrm{grad}\,T) = -k\,\Delta T$.
- $d_1 = (\sigma - \rho\frac{\partial\psi}{\partial\varepsilon}) : \dot{\varepsilon} - \rho\frac{\partial\psi}{\partial\alpha}\cdot\dot{\alpha}$ is the intrinsic dissipation; the 2nd principle specifies that d_1 is non-negative.
- $\rho T\frac{\partial^2\psi}{\partial T\partial\varepsilon} : \dot{\varepsilon} + \rho T\frac{\partial^2\psi}{\partial T\partial\alpha}\cdot\dot{\alpha}$ are the thermomehcanical coupling sources; the temperature variations induced by the fatigue loading are not large enough to modify the material state (no annealing induced by the self-heating). In other words, the coupling terms are limited to the thermoelastic sources induced by the material thermodilatability.
- r_e is the external volume heat supply. In the present experimental framework, r_e stands for the radiation energy per unit volume. The experimental arrangement tries to keep constant these radiation exchanges during a test.

2.2. Energy balance associated with a cyclic loading

Let us consider a thermodynamic process corresponding to a load–unload cycle whose the extreme states are named A and B. The first principle of thermodynamics can be locally written as [13–15]:

$$\rho\frac{\mathrm{d}e}{\mathrm{d}t} = \sigma : \dot{\varepsilon} + r_e - \mathrm{div}q = p_{\mathrm{def}} + r_e - \mathrm{div}q \quad (2)$$

Eqs. (1) and (2) integrated over the process duration $t_B - t_A$, lead, respectively, to:

$$\underbrace{\int_{t_A}^{t_B}\rho C\dot{T}\,\mathrm{d}\tau}_{\rho C(T_B - T_A)} + \underbrace{\int_{t_A}^{t_B}(\mathrm{div}(\vec{q}) - r_e)\,\mathrm{d}\tau}_{-Q_A^B} = \underbrace{\int_{t_A}^{t_B} d_1\,\mathrm{d}\tau}_{w_d} + \underbrace{\int_{t_A}^{t_B}\rho T\frac{\partial^2\psi}{\partial T\partial\varepsilon} : \dot{\varepsilon}\,\mathrm{d}\tau + \int_{t_A}^{t_B}\rho T\frac{\partial^2\psi}{\partial T\partial\alpha}\cdot\dot{\alpha}\,\mathrm{d}\tau}_{w_{\mathrm{tmc}}} \quad (3)$$

$$\underbrace{\int_{t_A}^{t_B}\rho\frac{\mathrm{d}e}{\mathrm{d}t}\mathrm{d}\tau}_{e_B - e_A} = \underbrace{\int_{t_A}^{t_B} p_{\mathrm{def}}\,\mathrm{d}\tau}_{w_{\mathrm{def}}} + \underbrace{\int_{t_A}^{t_B}(r_e - \mathrm{div}(\vec{q}))\mathrm{d}\tau}_{Q_A^B} \quad (4)$$

After some cycles, a symmetrization of heat losses can be observed so that the temperature variations become periodic over a cycle. The thermodynamic states A and B then verifies: $T_A = T_B$, $\sigma_A = \sigma_B$ and $\varepsilon_A = \varepsilon_B$. Combining Eqs. (3) and (4), allows writing the deformation energy spent over one cycle under the following form:

$$w_{\mathrm{def}} = (e_B - e_A) + w_d + w_{\mathrm{tmc}} \quad (5)$$

The temperature variations being small throughout the cycle, it has been shown in [10] that the contribution of the thermoelastic effects remains negligible, so that the deformation energy over a cycle is essentially made of internal energy variation and dissipated energy.

For uniaxial tensile-compression test, the deformation energy can be identified to the energy A_h associated with the area of the mechanical hysteresis loop, so that:

$$A_h = (e_B - e_A) + w_d \quad (6)$$

If now the internal energy variation over a cycle appears to be negligible, the mechanical cycle becomes a thermodynamic cycle where $\alpha_A \approx \alpha_B$. For such restrictive situation only the energy associated with the hysteresis area is transformed into dissipated heat:

$$A_h = w_d \quad (7)$$

3. Experimental setup

3.1. A simplified heat diffusion equation for materials with high diffusivity

Eq. (1) can be further simplified under the following hypothesis:

in the expression $\dot{T} = \frac{\partial T}{\partial t} + u\cdot\mathrm{grad}T$, the term $u\,\mathrm{grad}T$ can be neglected because the aluminium presents a high diffusivity coefficient inducing small temperature gradients (see Table 1); the radiation heat source r_e is supposed to be time-independent, so that $-k\Delta T_0 = r_e$, where T_0 is the equilibrium temperature field.

Under all these assumptions, the heat equation can be re-written in the following simplified, compact form:

$$\rho C\frac{\partial\theta}{\partial t} - k\Delta\theta = d_1 + s_{\mathrm{the}} = s \quad (8)$$

where $\theta = T - T_0$ stands for the temperature variation.

The aluminium alloy here considered has a high diffusivity coefficient (see Table 1) and this makes the estimation of heat source maps (2D distribution) or heat source profiles (1D distribution) a tricky problem because of the presence of second order derivation operator that must be applied to discrete and noisy temperature fields to estimate the local heat losses. In order to reduce at maximum the order of derivation, the following attitude was adopted which is consistent with a classical view of uniaxial tests. As stress and strain fields, we may suppose that, before the localization onset, the heat source distribution is uniform at any time within the specimen gauge part. In such a case, the spectral solution of the heat equation can be analytically determined by using the eigenfunctions of the Laplacian operator [2–10]. For symmetric linear boundary conditions and for initial conditions corresponding to uniform temperature fields, the spectral solution may then be well approximated by considering the only first eigenfunction. Then, the heat equation can then be simplified as

$$\rho C\left(\frac{\mathrm{d}\theta}{\mathrm{d}t} + \frac{\theta}{\tau_{\mathrm{eq}}}\right) \approx s \quad (9)$$

where τ_{eq} characterizes all the local heat losses and it is equal to 216 s for the considered alloy [10]. This equation can then be used to experimentally estimate the heat source, θ being identified to the mean temperature of a small volume.

Table 1
Thermophysical parameters of Al 2024 T3.

ρ	C	k	α_d
270 kg/m^3	*875 J/kg K*	120 W/mK	2.11×10^{-5} K^{-1}

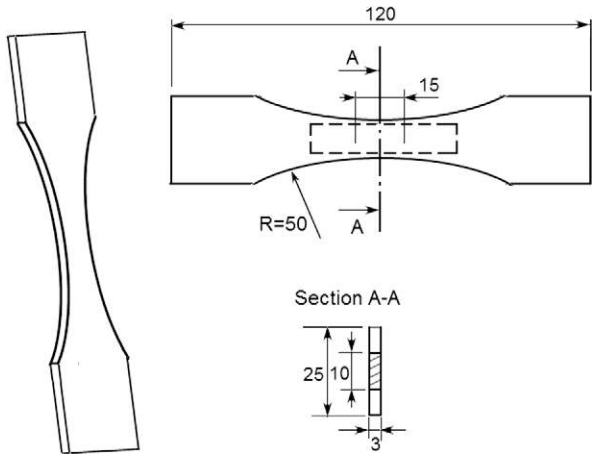

Fig. 1. 3D representation and dimensions of the specimen (with a dotted line is represented the zone of thermal data processing).

The fatigue specimen used in this work is shown in Fig. 1. The region, over which the temperature has been averaged, has been drawn with a dotted line.

Thin, flat specimens of Al 2024 T3 were tested with a MTS servo-hydraulic machine with load cell of 25 kN and applying a fatigue sinusoidal load at 17 Hz. One face of each specimen is prepared for IR acquisition with a uniform black and no-reflecting painting, while on the opposite face a speckle pattern is reproduced for successive image correlation.

The thermocamera employed for IR image acquisition is JADE-MW camera (CEDIP Infrared Systems); the acquisition rate is 9 Hz and images have a dimension of 320 × 240 pixels with a resolution of 0.3 mm/pixel. The CCD camera for acquisition of speckle images is CAMELIA 8 M (ATMEL) set with the following acquisition parameters: frequency of 4.5 Hz, window of 1023 × 280 pixels and with a resolution of 0.1 mm/pixel. The choice of load frequency and acquisition rate allows the sampled signals to be completely reproduced (see Fig. 2). A trigger is also used to synchronize the acquisition of the thermographic and speckle images.

In this section, two different approaches to evaluate dissipation sources are proposed on the basis of theoretical considerations exposed in Section 2.

3.2. Calculation of dissipation source evolution by temperature maps

It is demonstrated that the function describing thermoelasic source has the following form [1–5]:

$$s_{\text{the}} \approx -T_0 \alpha_{\text{d}} \dot{\sigma}_{11} \tag{10}$$

with α_{d}, coefficient of isotropic dilatation (see Table 1). For the particular oscillating load imposed, it means that s_{the} follows a sine trend; this implies that the total contribution of heat sources is composed by a sine part and a drift term that represents the pure irreversible dissipation.

Moreover the temperature signal is affected by noise and since the evaluation of sources passes through the computation of differential operators, the estimation of d_1 and s_{the} can result problematic for a bad SNR. In order to evaluate separately thermoelastic and dissipative contribution of heat source and, at the same time, to reduce the noise present in the signal, the temperature signal is locally fitted by last mean square method with the function:

$$\theta_{\text{app}}(x,y,t) = \underbrace{a\sin(2\pi f_s t) + b\cos(2\pi f_s t)}_{\theta_{\text{the}}} + \underbrace{ct + d}_{\theta_{d1}} \tag{11}$$

with a, b, c, and d, constants.

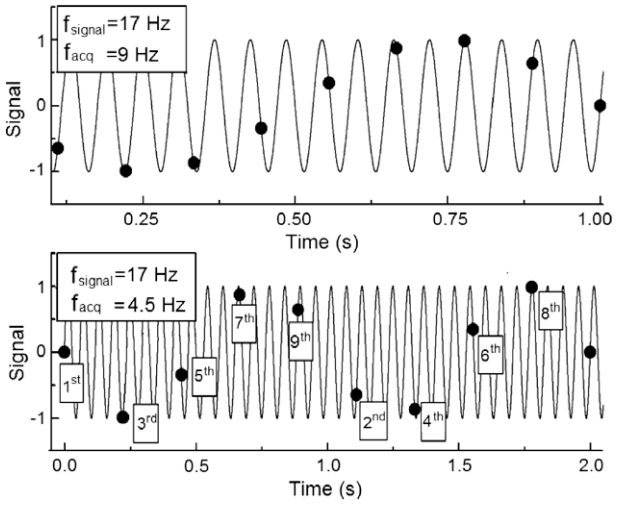

Fig. 2. Acquired points of a 17 Hz sinusoidal signal with a sampling rate of 9 and 4.5 Hz.

Under this condition, s_{the} and d_1 can be directly calculated employing, respectively, θ_{the} and θ_{d1} into Eqs. (2) and (3).

The values of sources are then divided by the constant quantity ρC for the alloy here considered and have dimension of K s^{-1} to have a more immediate idea of the heating rate.

3.3. Calculation of dissipation source evolution by digital image correlation

Digital image correlation (DIC) technique is here used to calculate the strain maps during each fatigue test and then to evaluate the dissipation source by Eq. (8); in fact considering that in two seconds (Δt) a specimen completes 34 cycles but the under-sampling condition (f_{acq} = 4.5 Hz) allows to re-build only one cycle (see Fig. 2) and identifying d_1 with its average value under the considered time interval, it is opportune to calculate the dissipation source, according to:

$$\frac{d_1}{\rho C} = \frac{1}{\rho C}\frac{A_{\text{hyst}}}{\Delta t} \tag{12}$$

First of all, the strain field is determined with DIC technique and the obtained values are averaged for the considered zone (see Fig. 1); then it is possible to calculate the stress with Hencky formulation, $\sigma(t) = \frac{\text{Force}}{\text{Section}} e^{\varepsilon(t)}$, and finally, after having identified every different cycle, it is possible to calculate A_{hyst}.

From now on, d_1^{the} and d_1^{DIC} represent the same physical quantity but evaluated with two different procedures.

3.4. Fatigue tests

Three tests with various loading blocks are here presented and for all of them a load ratio of 0.1 has been set.

In the first test, three blocks with decreasing level of load and a fourth block at $\sigma_{\max}$ = 440 MPa (very close to σ_{ult} for Al 2124 T3, equal to 480 MPa) are applied. The amplitude of thermoelastic contribution, Δs_{the}, and dissipation d_1^{the}, show a difference of three orders of magnitude (see Fig. 3a and b) and this peculiarity makes the elaboration for separating the two sources extremely difficult for the aluminium alloy. Considering that all tests exposed in this paper present a number of cycles low enough to allow damage to evolve into one single block and due to the necessity to improve the signal to noise ratio, the dissipation value are presented as averaged for each loading blocks.

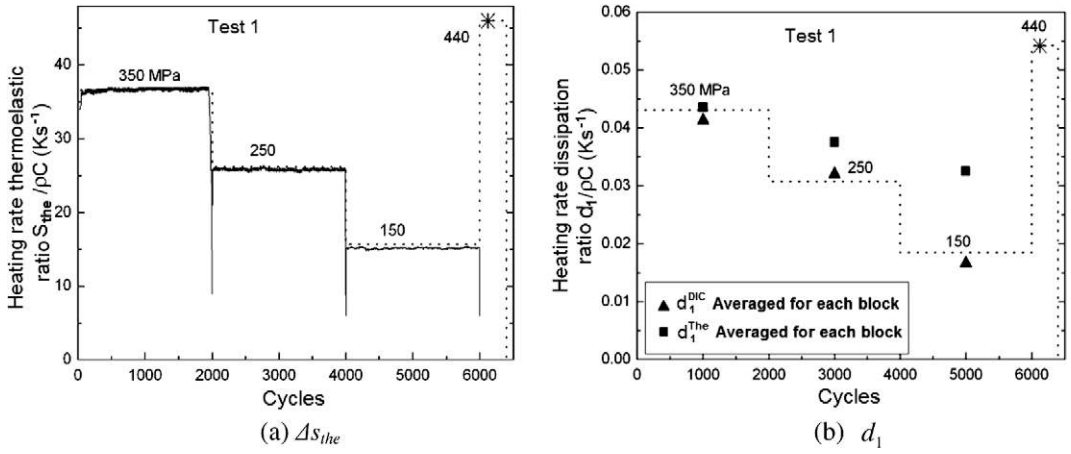

Fig. 3. Thermoelastic heating rate for test 1.

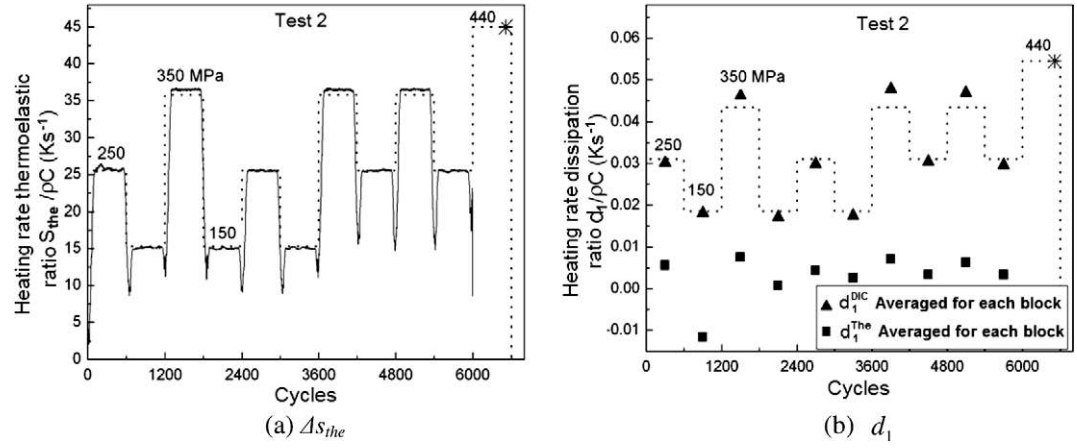

Fig. 4. Thermoelastic heating rate for test 2.

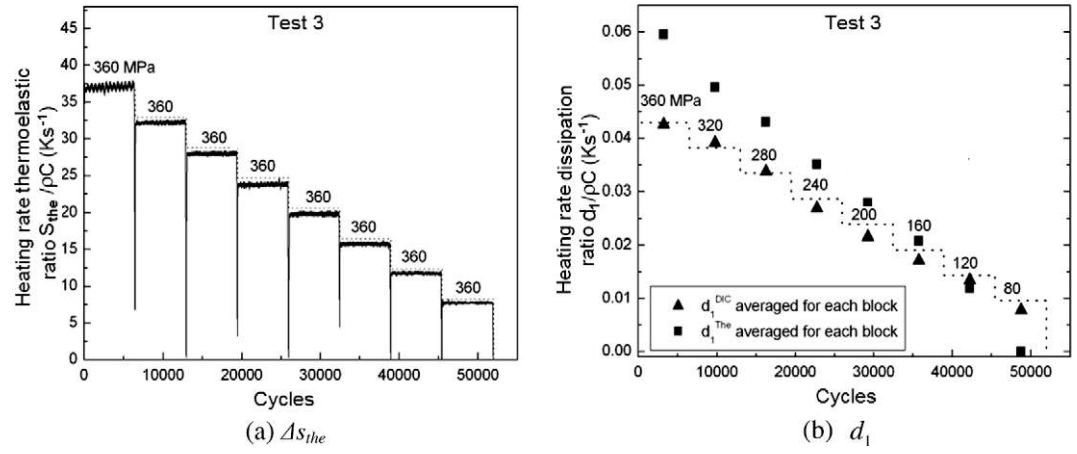

Fig. 5. Thermoelastic heating rate for test 3.

The result that emerges from the calculation of d_1^{DIC} (Fig. 3b) points out an important correspondence with d_1^{the} (Fig. 3b) either in terms of order of magnitude and either in terms of absolute values and this confirms the reliability of both the approaches employed to evaluate the dissipation source evolution. Unfortunately during the fourth block, in which failure occurs, the painting loses adherence to surface because of high deformations and image correlation has no more sense.

The test 2 presents 12 loading blocks, but in this case temperature data have a very low SNR (Fig. 4b) and sometimes elaboration shows negative values for dissipation sources, even if this has not any physical sense; on the contrary, Δs_{the} is worth of attention

(Fig. 4a). Dissipation d_1^{DIC} gives back information about the order of magnitude and values of dissipation that is in agreement with what emerges in first test.

In the third test eight blocks in a high–low sequence are, respectively, applied. The values of d_1^{DIC} for each block match with the ones calculated for the first and second test (see Fig. 5). The data extracted from temperature maps present a significant level of noise, anyway the evolution of dissipation is coherent with the application of growing loads. Finally, the graphs of d_1^{DIC} and d_1^{th} show a good proportionality with the applied load.

From the three experimental tests and relative data elaboration it emerges that final results depend significantly from the experimental conditions and preparation of specimen; in fact fragility of painting causes difficulty in image correlation algorithm, notwithstanding the two different methods of evaluation of the dissipation source evolution in time produce comparing and reliable results.

In the three tests, the measure of the amplitude of thermoelastic sources presents reliability and an excellent SNR.

The presence of noise characterizes the entire elaboration and surely represents a significant limit since sometimes its level overcomes the signal to measure. The bad signal to noise ratio also makes impossible a 1D or 2D elaboration for the particular studied aluminium alloy since the application of differential operators amplifies significantly the noise for both presented method.

The calculation of dissipation sources by means of image correlation represents an opportunity to evaluate damage evolution in time (as shown in this paper) and in space (it represents our actual work in progress).

4. Conclusions

Two different methodologies to estimate the evolution of dissipation sources were presented and compared: one is based on thermographic approach and the other on strain measurement by means of digital image correlation.

The material investigated is Al 2024 T3 that presents a high diffusivity and this provokes a difficulty to appreciate the dissipative contribution and separate it from the thermoelastic part of heat sources. Surely thermographic technique allows better results for steel alloy under fatigue, but under opportune and limiting conditions (considering heat sources uniform onto the entire specimen) information on time evolution of dissipation was here extracted for a aluminium alloy.

Starting from theoretical considerations it was possible to evaluate the evolution in time of dissipation sources from strain measurement so as derived by means of digital image correlation technique.

Digital image correlation is a affordable and versatile technique and what emerges in this paper is a interesting potentiality as monitoring of fatigue damage.

The presence of noise is a limiting factor that needs further attention to be optimized, but anyway it was possible to compare the performance of two methods. Surely the implementation of a filtering algorithm could allow to have spatial information about the damage and this can represent a possible objective to join.

References

[1] T. Boulanger, A. Chrysochoos, C. Mabru, A. Galtier, Calorimetric analysis of dissipative and thermoelastic effects associated with the fatigue behavior of steels, Int. J. Fatigue 26 (2004) 221–229.
[2] H. Louche, A. Chrysochoos, Thermal and dissipative effects accompanying Lüders band propagation, Mater. Sci. Eng. A 307 (2001) 15–22.
[3] A. Chrysochoos, Infrared thermography, a potential tool for analysing the material behavior, Mécanique Ind. 3 (2002) 3–14.
[4] B. Berthel, A. Chrysochoos, B. Wattrisse, A. Galtier, Infrared image processing for the calorimetric analysis of fatigue phenomena, Exp. Mech. 48 (2008) 79–90.
[5] S. Giancane, Studio a fatica della lega di alluminio 2024 T3 mediante termografia infrarossa e tecnica di correlazione di immagini, PhD thesis, Università di Lecce, Italy, 2006.
[6] B. Wattrisse, A. Chrysochoos, J.M. Muracciole, M. Némoz-Gaillard, Analysis of strain localization during tensile tests by digital image correlation, Exp. Mech. 41 (1) (2001) 29–39.
[7] B. Wattrisse, A. Chrysochoos, J.M. Muracciole, M. Némoz-Gaillard, Kinematic manifestations of localisation phenomena in steels by digital image correlation, Eur. J. Mech. A/Solids 20 (2001) 189–211.
[8] Y. Wang, A.M. Cuitiño, Full-field measurements of heterogeneous deformation patterns on polymeric foams using digital image correlation, Int. J. Solids Struct. 39 (2002) 3777–3796.
[9] B. Berthel, A. Galtier, B. Wattrisse, A. Chrysochoos, Thermographic analysis of fatigue dissipation properties of DP60 steel, Strain 43 (2007) 273–279.
[10] A.E. Morabito, A. Chrysochoos, V. Dattoma, U. Gallietti, Analysis of heat sources accompanying the fatigue of 2024 T3 aluminium alloys, Int. J. Fatigue 29 (2007) 977–984.
[11] P. Germain, Cours de mécanique des milieux continus, Masson, 1962.
[12] P. Germain, P. Muller, Introduction à la mécanique des milieux continus, Masson, 1986.
[13] J.L. Saurel, Etude thermomecanique d'une famille d'elastomeres thermoplastique, PhD thesis, Université de Montpellier II, France, 1999.
[14] R. Peyroux, A. Chrysochoos, C. Licht, M. Lobel, Thermomechanical coupling and pseudelasticity of shape memory alloys, Int. J. Eng. Sci. 36 (4) (1998) 489–509.
[15] A. Chrysochoos, B. Berthel, F. Latourte, S. Pagano, B. Wattrisse, B. Weber, 28 Local energy approach to fatigue of steel, Strain 44 (2008) 327–334.